The controversial role of inter-diffusion in glass alteration: Implications for Current Long-Term Modeling

S. Gin, L. Neill, M. Fournier, P. Frugier, T. Ducasse, M. Tribet, A. Abdelouas, B. Parruzot, J. Neeway, N. Wall

The Controversial Role of Inter-diffusion in Glass Alteration: Implications for Current Long-Term Modeling

S. Gin[1*], L. Neill[2], M. Fournier[1], P. Frugier[1], A. Abdelouas[3], B. Parruzot[2], J. Neeway[4], N. Wall[2]

[1] CEA, DEN, DTCD, SECM, F-30207 Bagnols-sur-Ceze, France.

[2] Washington State Univ, Dept Chem, Pullman, WA 99164 USA

[3] UMR 6457, Univ de Nantes, SUBATECH, Ecole Mines Nantes, CNRS, IN2P3, F-44307 Nantes 3, France

[4] Pacific NW Natl Lab, Energy & Environm Directorate, Richland, WA 99352 USA

Abstract

Current kinetic models for nuclear waste glasses (e.g. GM2001, GRAAL) are based on a set of mechanisms that have been generally agreed upon within the international waste glass community. These mechanisms are: hydration of the glass, ion exchange reactions (the two processes are referred as inter-diffusion), hydrolysis of the silicate network, and condensation/precipitation of partly or completely hydrolyzed species that produces a gel layer and crystalline phases on surface of the altered glass. Recently, a new idea with origins in the mineral dissolution community has been proposed that excludes inter-diffusion process as a potential rate-limiting mechanism. To understand how the so-called interfacial dissolution/precipitation model can change the current understanding of glass behavior, an in-depth review of the current knowledge with a special focus on inter-diffusion processes is considered. Also discussed is how experimental conditions change the predominant mechanisms and how one model may not be sufficient to explain the glass dissolution behavior under a wide range of geochemical conditions. In addition to the review of the above subjects, a key experiment used to account for the interfacial dissolution/precipitation model was replicated to further revisit the interpretation. It is concluded that the selected experiment design may lead to ambiguous conclusions and that, under the conditions investigated (dilute conditions, deionized water), evidence of inter-diffusion exists.

1. Introduction

The question of stability of silicate minerals and glasses over times is of importance in many sectors ranging from earth sciences to nuclear and pharmaceutical industries. From a manufacturering point of view, understanding the chemical durability of these materials is necessary to tailor their composition to their use. For instance, the dissolution rate of biomedical glasses must be determined to ensure delivery of the bioactive components to the proper biological system (Christie et al., 2016; Hench, 2006; Kokubo, 1991). Furthermore, understanding the alteration of basaltic glasses gives insight into global geochemical cycles of some key elements, storage of CO_2, or geological transformation of mars (Galeczka et al., 2014; Knowles et al., 2012; Minitti et al., 2007; Seyfried Jr et al., 1984). One important step to determining their behavior in a variety of systems whether biological or environmental is to understand their interaction with water (Conradt, 2008; Filgueras et al., 1993; Morin et al., 2015). Glass is also being considered as a containment matrix for high, intermediate, and low level radioactive waste arising from the reprocessing of spent nuclear fuel by many countries (Chaou et al., 2015; Ojovan and Lee, 2011; Pierce et al., 2008). The geological storage of nuclear waste in general, and glass in particular, is under consideration worldwide and it is admitted that the fate of radionuclides and their impact on the biosphere is strongly tied to waste forms alteration by ground waters. One major challenge in this field is to reliably demonstrate the safety of the disposal over the next hundreds of thousands of years (Gin et al., 2013a; Grambow, 2006; Vernaz and Dussossoy, 1992).

One approach to develop predictive mechanistic models has been designed by the scientific community (ASTM International, 2008; Campbell and Cranwell, 1988; Poinssot and Gin, 2012). Initially, mechanistic and parametric studies are designed to understand basic processes. By coupling various conditions and progressively considering realistic conditions, experiments and in-depth characterization of altered glass samples allow the determination of the key processes that must be captured by the model. Mechanistic kinetic models are then developed to interpret experimental data with increasing complexity and eventually extrapolate long-term behavior under repository conditions. One method to validate models is the study of natural or archeological glasses that have been subjected to a variety of conditions for periods exceeding the human timeframe (Libourel et al., 2011; Techer et al., 2000; Verney-Carron et al., 2008).

Several models are currently being used to assess the long-term stability of these waste forms, such as GM2001 (Grambow and Müller, 2001), GRAAL (Frugier et al., 2008) and more simpler rate laws derived from the general equation given by Lasaga et al. (1995). Recently, a new theory initially built for silicate minerals (Hellmann et al. (2012) and references therein) was extended to silicate glasses based on specific observations (Geisler et al., 2015; Hellmann et al., 2015). This theory suggests that both silicate minerals and glasses dissolve congruently within a thin interfacial film of water and alteration products then form by precipitation from

species released in this film. This idea is supported by many observations of cross sections of alteration rims formed on silicate minerals, which show sharp chemical gradients of species that were once assumed to diffuse (Hellmann et al., 2012). In the attempt to generalize the theory to glass, Hellmann et al., 2015 characterized with Atom Probe Tomography (APT), Transmission Electron Microscopy (TEM) and Time-of-Flight Secondary Ion Mass Spectrometry (ToF-SIMS) samples of SON68 glass (composition given in Table 1) – the inactive surrogate of the French R7T7 glass fabricated at the La Hague facility for high-level waste arising from spent nuclear fuel reprocessing – altered at 50°C in very dilute conditions (Hellmann et al., 2015). The observation of sharp gradients for highly mobile species, such as B and Na, led to the assumption by the authors to neglect the commonly described process of inter-diffusion in any cases (water diffusion in the glass and ion exchange). This present review attempts to understand how this interfacial dissolution/precipitation idea presented recently by a few authors fits in with the observations and with the currently accepted waste glass corrosion models. The experiment discussed by Hellmann et al. (2015) – and referred as “Hellmann et al.’s experiment” in the following – has been replicated to re-examine their results.

2. Fundamentals in Glass Alteration

2.1 Glass Structure

As the dissolution/precipitation idea is inherited from many observations performed on silicate minerals before being generalized to silicate glasses, it is important to consider what defines a glass. Glass is essentially a solid that is cooled at such a rate that large-scale crystallization is inhibited by its viscosity. Compared to crystals, a glass only keeps short range (2–5 Å) or medium range (5-20 Å) order in regards to the network forming elements (Elliott, 1991; Zachariasen, 1932). In addition to the network forming elements (Si and B in our case), additional elements can be included to modify the glass network connectivity. Glass modifiers such as alkali and alkaline earth elements depolymerize the network acting as charge compensators for non-bridging oxygen or other unbalanced species of intermediate elements (e.g. Al, Zr, Fe, Zn, Mo). These intermediate elements can strengthen or loosen the overall structure depending on the global composition of the glass (Calas et al., 1987; Stebbins and Xu, 1997). This ability to change the physical (melting temperature, viscosity, electrical resistivity, etc.) and chemical properties by the addition of multiple elements allows glass to be tailored to a variety of applications including the storage of nuclear waste. The composition of borosilicate glasses used in nuclear waste conditioning are typically made of ~20 to ~40 of oxides with a waste loading capacity of about 15-35 wt%. This advantage is counterbalanced by two major limitations: (i) compared to silicate minerals the glass structure is more open allowing water to slowly diffuse in (Bunker, 1994; Davis and Tomozawa, 1995) and (ii) a thermodynamic

equilibrium between glass and solution cannot be achieved (Grambow, 1985). Thus, in contact with water, glass undergoes irreversible transformations into more stable phases. In this paper we mainly focus on SON68 glass as (i) it was the glass studied by Hellmann et al. (2015) and (ii) it is the most studied simulant nuclear glass to date.

2.2 Mechanisms and Kinetics of Glass Alteration

2.2.1 Mechanisms of Glass Alteration

A general set of mechanisms and kinetic regimes have been agreed upon to describe the interaction between borosilicate glasses and an initially dilute aqueous medium (Conradt, 2008; Vienna et al., 2013). Understanding of glass corrosion arises from correlating solid characterization with solution data. These correlations allow rate controlling steps and the corresponding kinetic regimes to be determined. The initial stage of glass dissolution in deionized water is represented by several coupled mechanisms (Bunker, 1994); hydration by water diffusion in the glass structure (Doremus, 1975; Rébiscoul et al., 2007; Rébiscoul et al., 2004; Smets and Lommen, 1983) and the ion-exchange of the alkali ions of the glass surface with hydronium ions in solution (Angeli et al., 2001; Boksay et al., 1967; Doremus, 1983; McGrail et al., 2001; Ojovan et al., 2006; Rebiscoul et al., 2003) as shown in equation 1 where M^+ is an alkali ion.

$$\equiv Si\text{-}O^{-}\cdots M^{+} + H_3O^{+} \rightarrow \equiv Si\text{-}OH + M^{+} + H_2O \qquad \text{Equation 1}$$

Note that water diffuses in the glass as an intact molecular species only through large rings made of at least six silica tetrahedrons (Bunker, 1994). As glasses of nuclear interest are dense and highly polymerized, they do not contain many large rings, thus ion-exchange dominates the first stage of nuclear glass alteration. McGrail et al. (2001) suggests that water dissociation could be the rate-limiting step controlling ion exchange. Moreover, it is often seen that B is released along with alkali. Although B is a glass former, the fast hydrolysis, associated to a low energy barrier for breaking B-O-Si bond, can explain this behavior. In the following, water diffusion through the glass, ion exchange and hydrolysis of B are gathered under the general term of inter-diffusion. These reactions cause the pH of the system to rise, thus leading to the dissolution of the glass network, which corresponds to the hydrolysis of the Si-O-X (X = Si, Al, Fe…) bonds (Hench and Clark, 1978; Techer et al., 2001):

$$\equiv Si\text{-}O\text{-}X + OH^{-} \rightarrow \equiv Si\text{-}O^{-} + \text{-}X\text{-}OH \qquad \text{Equation 2}$$

$$\equiv Si\text{-}O\text{-}X + H_2O \rightarrow \equiv Si\text{-}OH + \text{-}X\text{-}OH \qquad \text{Equation 3}$$

The hydrolysis of the four ≡Si-O-X bonds leads to the release of orthosilicic acid and potentially the ‘X species’ into the solution. When the concentrations of silica and X species in solution

increase, concurrent reactions of precipitation and in situ condensation occurs (Iler, 1979). These mechanisms are shown for silica in equations 4, 5, and 6.

$$\equiv Si\text{-}OH + \equiv Si\text{-}OH \leftrightarrow \equiv Si\text{-}O\text{-}Si\equiv + H_2O \qquad \text{Equation 4}$$

$$H_4SiO_4 + \equiv Si\text{-}OH \leftrightarrow \equiv Si\text{-}O\text{-}Si(OH)_3 + H_2O \qquad \text{Equation 5}$$

$$H_4SiO_4 + H_4SiO_4 \leftrightarrow 2SiO_2 + 4H_2O \qquad \text{Equation 6}$$

The concentration of silica eventually reaches steady state, when hydrolysis and precipitation and/or condensation rates are equal. The elements that strongly interact with Si, such as Al, Ca, Fe, Zr can change this steady state due to their influence on dissolution and condensation/precipitation rates.

2.2.1 Kinetics of Glass Alteration

Theoretically all the reactions cited above compete during glass alteration but the rates of each are dependent on factors such as glass composition (Frugier et al., 2005; Gin et al., 2012; McGrail et al., 2001), temperature (Calligan and Pierce, 2007; Knauss et al., 1989; Pierce et al., 2008), and pH (Advocat et al., 1991; Inagaki et al., 2013; Werme et al., 1983). As a result, each of them can be rate-limiting depending on the experimental conditions. For instance, while the solution conditions are still dilute and the pH close to neutral, there is no backward reaction of silica and glass alteration is limited by the hydrolysis of the silicate network. The resulting rate is called the initial or forward rate; this is the maximum dissolution rate for a given temperature and pH and characterized by a nearly congruent glass components release. As Si concentrations increase in the solution, the rate of hydrolysis of the silicate network decreases and backward reactions take place. As a result, porous, amorphous, and hydrated compound called the *gel* forms on the glass surface by precipitation and in situ condensation (Gin et al., 2015a; Grambow, 1985; Jégou et al., 2000; Valle et al., 2010). Note that the gel is not a pure silica polymorph. SON68 glass, as well as most of nuclear glass compositions contain many low solubility elements that can bound to Si-O such as Fe, Al, Zr and Ca. As a result the gel can accommodate a number of cations released from the glass or coming from the solution.

The residual rate regime is believed to begin when the solution has reached a steady state concentration of Si in solution but ion exchange may still occur (Gin et al., 2012; McGrail et al., 2001; Petit et al., 1990a). There was debate on whether the rate drop is due to the buildup of glass components (effect of limiting transport through the gel layer) or due to the diminishing affinity of the dissolution of the silicate network. This debate ended in the 2000's when it was determined that both affinity and transport of reactive species through the gel affect the glass dissolution rate (Van Iseghem et al., 2009). One theory suggests that if the gel is sufficiently dense it can be passivating, meaning that the diffusion coefficient of the mobile species through

it is smaller than the inter-diffusion coefficient in the pristine glass (Gin et al., 2013c; Parruzot et al., 2015). The corresponding rate is then controlled by reactive diffusion of water through the passivating layer and the precipitation of secondary phases that take up the elements from the passivating layer. When precipitation of aluminosilicate phases is sufficiently large, in the case of zeolite under hyper alkaline solutions, glass dissolution can suddenly resume and go back to the initial conditions reflecting the pH of the contacting solution and experimental temperature (Ebert and Bates, 1993; Fournier et al., 2014a; Ribet and Gin, 2004).

2.2.3 Alteration products

The set of reactions described above lead to the formation of amorphous and crystalline phases on the glass surface. Figure 1a displays the different alteration products described by the classical theory involving inter-diffusion. Figure 1b shows the same materials interpreted by the interfacial dissolution/precipitation model. The stack of amorphous and more or less crystalline phases can be explained by the Ostwald rule of stages (Ostwald, 1897). This rule states that a system will go through a series of intermediate steps to eventually reach the most stable one; the least stable step will be formed first for kinetic reasons while the most thermodynamically favored will be formed last (Threlfall, 2003). This is also observed for natural glasses altered both in the laboratory or in the field (basaltic glass) as gel-like materials form first followed by the precipitation of clays minerals and much later by zeolites (Crovisier et al., 2003). As a whole, and whatever the theory for glass alteration, the role of alteration products on glass dissolution kinetics is of primary importance because they control either the solution chemistry (Curti et al., 2006; Fournier et al., 2014b; Strachan and Neeway, 2014; Vienna et al., 2013) or limit the transport of aqueous species (Cailleteau et al., 2008; Gin et al., 2011; Gin et al., 2015a; Jollivet et al., 2008; Rébiscoul et al., 2005; Rébiscoul et al., 2004) and can, in the case of massive precipitation of zeolites, sustain glass alteration at a high dissolution rate.

2.3 Advancements in Models

Attempts to build rate laws date back to the 1980's with the pioneering work of Aagaard and Helgeson (1982) based on the transition state theory. This theoretical framework was then used by (Grambow, 1985) to derive a first-order rate law to explain why the glass dissolution rate drops. In this model, the hydrolysis of the fourth Si-O-X bond once the three others have been hydrolyzed, is supposed to be the rate limiting step controlling the whole glass dissolution process. The glass dissolution rate is then:

$$r = r_0 \left(1 - \frac{a(\mathrm{H_4SiO_4})}{K}\right) \qquad \text{Equation 7}$$

Where r_0 is the initial dissolution rate, $a(H_4SiO_4)$ the activity of orthosilicic acid, K the pseudo equilibrium constant for the hydrated glass.

Over time, additional models have been devised to take into account the effect of the alteration layers (Bourcier et al., 1989; Daux et al., 1997; Munier and Crovisier, 2003). The corresponding models assume that the glass dissolution rate is controlled by the equilibrium between the gel and the solution. Experimental evidence of transport-limiting properties of dense gels accumulated in the late 1990's and, new models were developed. GM2001 (Grambow and Müller, 2001) couples an affinity-based rate law between the glass and dissolved silica and the diffusion of Si and H_2O through the gel (Ferrand et al., 2006). The affinity term is based on the activity of H_4SiO_4 in solution and a corresponding saturation constant K_{SiO2} at the dissolving glass surface. In this model, the formation of the gel is due to the precipitation of silica following its dissolution from the glass network. Another advanced model designated GRAAL for Glass Alteration with Allowance for the Alteration Layer, assumes that the glass dissolution rate is dependent on the diffusion properties of a dense altered layer designated as the PRI or passivating reactive interphase (Frugier et al., 2008). The PRI forms by water diffusion into the glass, ion exchange and self-reorganization. It then transforms by dissolution/precipitation into a porous, non-passivating gel and secondary phases. The PRI and the the gel are modelled by a set of 6 end-members whose composition and solubility have been empirically determined (Rajmohan et al., 2010). Until now, GRAAL is the only model that is able to calculate residual rate without the use of fitting parameters (Frugier et al., 2009; Gin et al., 2013b) although the range of conditions in which the model is applicable is still narrow (SON68 glass, 50°C or 90°C, pH 6-10).

The Monte Carlo method has also been used to understand the mechanisms of glass-water reactions. Although this method is simplified from the variety of factors that influence the rates and mechanism seen during glass alteration it has given insights into the interfacial reactions and properties of the alteration layer. This computational method assumes the glass structure as a lattice where the lattice points are the glass formers Si, Al, and B. The modifier ions, alkalis and alkaline earths, are placed at interstitial positions. This method uses overall probabilities (dissolution, precipitation) for each of the different glass components. This method has been used successfully to understand the morphological changes within the alteration layer (Cailleteau et al., 2008; Cailleteau et al., 2011; Ledieu et al., 2004), changes due to glass-surface-area-to-solution-volume ratio (*S/V*) and glass composition (Devreux et al., 2004), and solution effects (Santra et al., 1998). Initially, only pore clogging accounted for the rate decrease, but a diffusion term was recently introduced into the model that greatly enhanced the method's ability to model glass behavior (Kerisit et al., 2015).

As explained above, in the last few years, the current understanding of glass alteration mechanisms has been challenged by a new idea arising from mineral and ceramic science (Geisler et al., 2015; Hellmann et al., 2015; Hellmann et al., 2012). This idea stresses the importance of a thin film of water that is assumed to be present on the surface of the pristine glass/aqueous interface and how the characteristics of this region differ from the bulk solution. As the glass alters, saturation takes place in this thin water film that causes the precipitation of an alteration layer (Figure 1b). Here, the extent of alteration is not due to bulk solution saturation in silica but in the solubility difference between amorphous silica within the interfacial fluid and the silica within the glass network. The whole alteration layer is thus considered as a precipitate. As all the glass constituents are supposed to dissolve congruently in the thin film of water, no chemical gradients form at the interface and both water diffusion in the glass and ion exchange are thus supposed to be negligible. According to the authors, the absence of chemical gradients at the glass/alteration layer interface would give enough credit to this new theory and allows them to generalize it to all experimental conditions. At this stage, this new idea only relies on observations; no equations are available that could be compared to experimental data.

The following discussion delves deeper into our current understanding of these models, how the proposed idea of interfacial dissolution/precipitation fits with current data, a discussion of the role of inter-diffusion within the various surface layers, and the points that must be further understood to create models that can accurately predict the behavior of glass waste over geological time scale.

3. Understanding Alteration Layers Formation in relation with Inter-diffusion

3.1 Evidence of ion exchange processes at low reaction progress

Advocat et al. (Advocat et al., 1991; Advocat et al., 1990) performed dissolution experiments of SON68 glass specimens at 90°C in dilute conditions (low surface-to-volume ratio), under acidic, neutral and basic conditions and short durations (typically a few days) in order to avoid affinity effects and other backward reaction. These conditions are the best to understand the effect of pH on the basic mechanisms (mainly ion exchange and hydrolysis) in the absence of alteration layers. Moreover the experiment performed in deionized water at low S/V ratio is of great interest because it corresponds to the very first stages of the Hellmann et al.'s experiment. The difference in temperature between the two studies (90°C for Advocat et al.'s study versus 50°C for Hellmann et al.'s experiment) does not change the conclusion. The series of experiments reported by Advocat et al. clearly show that lower the pH results in faster Na and B release compared to Si. This incongruency is clearly visible below pH 7 at 90°C (Figure 4 in Advocat et

al. (1991)). Moreover, below pH 7, Na is released slightly faster than B, showing that, as expected, the exchange reaction H_3O^+/Na^+ is faster than the dissolution of B-O-X (X = B, Si, Al) bonds. In deionized water the preferential release of Na and B lasts about 2 days, and the resulting depleted layer is approximately 30 nm thick. Under acidic conditions, at pH 2, this depleted layer exceeds 3000 nm. These results cannot be explained by the interfacial dissolution/precipitation model as silica concentrations are far from saturation whatever the pH, thus silica cannot precipitate in these conditions (solubility of amorphous silica at 90°C pH ranging from 2 to 8 is about 140 $mg.L^{-1}$ of Si_{aq}). The best evidence is provided by the experiments at pH 8 and above where the dissolution of Si, Na and B is congruent, showing that silica does not precipitate. These experiments thus strongly support the classical theory where inter-diffusion (i.e. ion exchange and fast dissolution of boron) on the one hand and hydrolysis of the silicate network on the other hand compete because of the difference in the bonding energy between glass cations and oxygen atoms. As a result of these competing reactions, a Na and B depleted and hydrated layer, also called leached layer, hydrated glass or gel depending on the authors, forms on the glass at low reaction progress, at least in acidic and slightly alkaline pH conditions.

3.2 From the hydrated glass to the gel layer formed at high reaction progress

Regarding the formation and growth of the gel layer, two theories are commonly proposed. One is based on precipitation due to saturation of the bulk solution (Crovisier et al., 1987) and another is based on the in-situ condensation of partly dissolved Si-O-X (X = Si, Al, Zr, Fe…) bonds (Bunker, 1994; Gin et al., 2001). Recent studies using Si isotopes show that both reactions take place, their relative importance depends on the deviation from saturation (Geisler et al., 2015; Gin et al., 2015a; Gin et al., 2015b; Valle et al., 2010). It is seen that a diluted solution (i.e. low concentration of silica) favors a complete detachment of Si atoms bound to the glass and further precipitation of dissolved silica once the concentration achieves saturation.

It is thought that if the gel is protective, transport of reactive species (water molecules, hydroxyl and hydronium ions) is slowed down as well as the transport of species released from the glass (Gin and Mestre, 2001; Leturcq et al., 1999; Pierce and Bacon, 2011; Rébiscoul et al., 2005; Vernaz and Dussossoy, 1992). As a consequence chemical gradients should take place within the layer.

These gradients have been characterized by multiple analytical techniques such as Time of Flight – Secondary Ion Mass Spectrometry (ToF-SIMS) and more rarely with Nano-SIMS, Atom Probe Tomography (APT), Transmission Electron Microscopy (TEM), or Rutherford Backscattering Spectroscopy (RBS). It is commonly seen that, at high reaction progress, elements such as B, Na, and Ca display similar gradients which are anti-correlated with H

(Chave et al., 2011; Gin et al., 2011; Gin et al., 2015a; Gin et al., 2015b; Maeda et al., 2012; Petit et al., 1990b). For SON68, these gradients are sharp and only located near the pristine glass / hydrated glass interface (Gin et al., 2011). Although B does not undergo ion exchange, its high mobility is attributed to the fast dissolution of the B-O-X bonds due to a much lower energy barrier than for Si-O-Si (Zapol et al., 2013). Interestingly, as B, Na, and Ca are not bound similarly to O atoms in the glass structure, in can be inferred from the observation that the three cations display similar profiles in the alteration layer that the rate-limiting process is rather the water transport through the alteration layer than the detachment of the glass species. This is in agreement with previous works (Ferrand et al., 2006; Frugier et al., 2008). Hellmann et al. (2015) showed much sharper profiles by APT than by ToF-SIMS and TEM and used that observation to conclude that inter-diffusion is negligible. One can wonder if this observation is sufficient to build a new theory for glass dissolution excluding inter-diffusion.

3.3 Diffusion coefficients for SON68-type glasses at low and high reaction progress

Table 2 shows a comparison of multiple apparent diffusion coefficients under a variety of conditions and the methods of analysis. When comparing the diffusion coefficients, differences can be seen even when comparing the same element determined by the same method. So what causes these differences?

The penetration of water into the glass surface depends on glass composition, pH and temperature (Rébiscoul et al., 2012). As an example, the water diffusion coefficient (D_w) measured at pH = 3 at 30 °C were seen to change between 1.1 x 10^{-19} to 4.6 x 10^{-21} $m^2.s^{-1}$ based on varying concentrations of calcium within the glass composition. These diffusion coefficients were measured at the initial stages of glass alteration. For SON68 glass D_w expected in the early stage of the experiments by Hellmann et al. (2015) (50°C, near neutral pH) is about 10^{-21} $m^2.s^{-1}$ (Rébiscoul et al., 2007). It is worth noting that He, an atom of the same size as a water molecule, but not involved in chemical reactions with glass species, diffuses in SON68 glass at the same temperature with a diffusion coefficient 10^5 greater than water (Chamssedine et al., 2010). This result suggests that water transport in the glass is not only tied to topological features (e.g. density of large rings) but also to chemical reactivity (dissociation, ion exchange, hydrolysis reactions, formation of silanol groups, solvation reactions…). The way water reacts with glass components has never been accurately taken into account in the different inter-diffusion models.

At higher reaction progress, still at 50°C and near neutral pH, D_w is one to two orders order of magnitude lower (10^{-22}-10^{-23} m^2 in Ferrand et al. (2006)). This effect, also seen for basaltic glass (Parruzot et al., 2015) may be attributed to the protective properties of the PRI (Gin et al., 2013b; Gin et al., 2015a). However, the way the gel limits the apparent diffusion coefficient of

water remains to be clarified. The values of D_w are related to solid-state diffusion as transport in porous media cannot account for such low values. As a consequence, the chemical gradients of B, Na, Ca, as evidenced by ToF-SIMS do not correspond to detached species from the glass that are moving through the gel in the liquid phase but rather to a uneven reactive front whose shape depends on how fast water molecules arrive and react with glass species. A simple argument supporting this idea is that samples re-analyzed by ToF-SIMS several months after the first analysis display exactly the same profiles (not shown here). In the case of an aqueous species diffusing within the porosity, the corresponding profiles would have change dramatically.

4. Importance of Experimental Conditions

4.1 Recreating Experimental Conditions Supporting the Interfacial Dissolution/Precipitation Model

In the hopes of further understanding the processes seen in Hellmann et al. (2015), a similar experiment was performed and analyzed by TOF-SIMS to compare the diffusion profiles gained under this set of conditions. The only difference between the two protocols is that our reactor was not stirred. Indeed, we highlight the importance of stirring in this experimental setup because, at the relatively low temperature of 50 °C and low *S*/*V* ratio, if the solution is not stirred, local chemical gradients in the solution may exist and this will affect the determination of the results.

4.1.1 Materials and Methods

The glass studied in this work is SON68. All experiments are carried out in a static system in 180 mL PFA reactors. The initial leaching solution is 18 mΩ.cm deionized water and the pH is allowed to float throughout the experiment while keeping the temperature constant at 50 °C. The glass is prepared in monolith form with the dimensions of 2.5 cm x 2.5 cm x 0.2 cm and the two main faces are polished with SiC papers and finally with diamond paste of 1 µm. One SON68 monolith is used per reactor with a solution volume of 145 mL giving a glass-surface-to-solution-volume ratio of 0.1 cm^{-1}. This experiment is performed in triplicate. Solution aliquots are taken for all experiments at day 1, 4, 7, 14, 29, and 180. The aliquots are filtered with 45 µm filters and acidified with 0.5 M HNO_3 prior to analysis by ICP-AES. The pH values are also taken at the same time durations and are recorded at the experimental temperature of 50 °C.

Time-of-Flight Secondary Ion Mass Spectrometer (ToF-SIMS) (TOF.SIMS5, IONTOF GmbH®, Münster, Germany) is used to determine the elemental depth profiles on the glass coupon altered 180 days. In this case, the crater was 200 × 200 μm^2 and the rastered area is 60 × 60 μm^2 (256 x 256 pixels). The analysis is performed with a 1-keV, 290-nA sputter beam of O_2^+ to

detect positive species. The depth of the crater is measured after the analyses and profiles are calculated assuming that the sputtering rate is constant. Post treatment of the data is performed to calculate the chemical profiles of B and Li in areas of 30 x 30 µm, 15 x 15 µm, 7.5 x 7.5 µm and 3.75 x 3.75 µm within the 60 x 60 µm area. Although the signal-to-noise ratio diminishes with the decrease of the selected area, this investigation helps identify the existence of a mixing zone at the corrosion front due to a rough interface or an uneven alteration layer (Figure 2a).

4.1.2 Results and Discussion

Table 3 shows the solution data of our unstirred experiment compared to the results in Hellmann et al.'s experiment. The results from the two experiments are in general agreement, although there is a large error associated with running the experiment in triplicate, which likely comes from the extremely dilute conditions. Under these conditions, the solution analysis is near the limit of detection for the ICP-AES instrumentation, thus the error is increased. This error is also seen in the pH of the solution. The values remain close to neutral pH, however such measurements are made difficult in low ionic strength conditions.

We have also compared these results to a series of experiments performed at CEA in the 1990s under stirring conditions (Advocat et al., 1993). As the S/V ratios were slightly different (0.24 cm^{-1} for CEA stirred experiment and 0.1 cm^{-1} for Hellmann et al.'s experiment) concentrations are normalized to get equivalent thicknesses of altered glass (Equation 7):

$$ETh(i) = \frac{C(i)}{S/V x_i \rho} \qquad \text{Equation 8}$$

where *C(i)* is the concentration of *i* (*i* = B, Si) in the solution, *S/V* the surface area to solution volume ratio, x_i the mass fraction of *i* in the glass (x_B = 4.35, x_{Si} = 21.25), and ρ the density of the glass (2.75 $g.cm^{-3}$).

Figure 3 shows the comparison between the two sets of experiments. It appears that in solutions homogenized by stirring, glass is 3 to 4 times more altered after 20 days of experiment than without stirring. Moreover dissolution is almost congruent in homogenous solution whereas without stirring *ETh*(Si) is about one fourth of that of *ETh*(B) meaning that about 75% of Si is retained in the alteration products. This comparison and the fact that the results of our unstirred experiment are very similar to those of the Hellmann et al.'s experiment, strongly suggest that contrarily to what is stated in Hellmann et al. (2015), the solution was not stirred. In unstirred solutions, concentrations are higher near the glass surface, increasing condensation and precipitation of silica depending on local concentration. As a result, it is unsure that alteration proceeds at the same rate everywhere on the glass coupon. With such a limitation, the discussion of the results from Hellmann et al. (2015) becomes more speculative. For instance,

alteration thicknesses derived from B concentrations are much greater than thicknesses of gel, e_{gel}, measured by TEM (after one month *ETh*(B) = 120 nm and e_{gel} = 55 nm; after 7 months *ETh*(B) = 220 nm and e_{gel} = 80 nm); this could be due to gel shrinkage during sample preparation (Gin et al., 2001; Rébiscoul, 2004), retreat of the initial interface during alteration (Icenhower and Steefel, 2013) but it cannot exclude large variations in gel thickness due to local chemical conditions. This might expand the mixing zone (Figure 2a) and thus the width of the gradient area measured by ToF-SIMS.

Figure 2 displays B and Li ToF-SIMS profiles for the 180 day altered sample retrieved from the unstirred solution. The interface is located around 180-200 nm below the surface in good agreement with the solution data but not with TEM data. Both B and Li display the same profiles with a sharp decrease from the pristine glass up to a normalized concentration of about 0.2. Beyond this value the concentration slowly decreases down to 0. It is clear that B and Li gradients are larger when derived from the 60 x 60 µm rastered area than for smaller zones. However the gradients seem to be the same when calculated from 30 x 30 µm or smaller areas. This means that B and Li profiles are not adversely expanded by a rough interface or an uneven alteration layer, at least in the probed area. According to that, it could be said that B and Li interfacial gradients (measured between 20% and 80% of the pristine glass concentration) are ~23 and ~17 nm, respectively. Note that with the global signal obtained from the 60 x 60 rastered area, B and Li interfacial gradient are approximately doubled. With the 100 x 100 µm rastered area used by Hellmann et al, 2015 gradients are even larger (around 75 nm if one assumes that 300 s of sputtering corresponds to 200 nm of sputtered material).

Despite caution in interpreting ToF-SIMS profiles is taken, interfacial gradients of ~20 nm are still greater than those reported determined by APT by Hellmann et al., 2015 (2-5 nm). Although APT shows that there is a sharp decrease of B and Li concentration at the so-called dissolution-precipitation interface (Figure 2b of Hellmann et al. (2015)), concentration of these two elements are lower between 0 and 20-30 nm than further in the pristine glass. Unfortunately no exogenous elements such as K or Cl or H are displayed, making the precise location of the pristine glass/alteration layer interface a somewhat arbitrary assignment. Regarding B profiles derived from EFTEM images (Figure S1 of Hellmann et al. (2015)), gradient' widths cannot be calculated accurately because of the low signal-to-noise ratios. Consequently, none of the techniques applied to the sample can irrefutably demonstrate that no diffusion layer of a few tens of nanometers forms under the tested conditions.

The thickness of the diffusion zone given by this new ToF-SIMS analysis is in agreement with what can be estimated by an approximate calculation based on the Fick's second law. Indeed, with the assumption that, in the steady state, the ingress rates of the inter-diffusion and

hydrolysis fronts are equalized, the thickness of the diffusion zone can then be simply approximated by equation 9 with D the apparent inter-diffusion coefficient ($m^2.s^{-1}$) and r the ingress rate of the dissolution front ($m.s^{-1}$).

$$e \approx \frac{D}{r} \qquad \text{Equation 9}$$

r is calculated from boron solution concentrations. D is evaluated according to equation 10 with $D_0 = 7.99 \cdot 10^{12}$ $m^2 \cdot s^{-1}$, $n = 0.65$ and an activation energy $E_a = 94.7$ $kJ \cdot mol^{-1}$. The variations of the inter-diffusion coefficient with pH and temperature were described by (Chave et al., 2007) and recalculated for pH values ranging from 6 to 10 by (Jollivet et al., 2012).

$$D = D_0 \times [\mathrm{HO^-}]^n \times \exp\left(-\frac{E_a}{R \times T}\right) \qquad \text{Equation 10}$$

Boron concentrations and pH values were obtained from data provided by Hellmann et al. (2015) (Figure 4a, b) and the calculation leads to a thickness of the inter-diffusion zone of ≈ 10 nm after 180 days (Figure 4c) of the same order of magnitude as that obtained by ToF-SIMS in our experiment. It appears that the experimental conditions in Hellmann et al.'s study are not suitable to form a thick inter-diffusion zone, unlike the conditions employed in an study focused on this aspect, for example, by Gin et al. : 90°C, pH 7 and a solution saturated with silicon (Gin et al., 2015a), in which 1-µm thick hydrated glass layer was formed after a few months.

4.2 Other experimental evidences challenging the interfacial dissolution/precipitation model in near neutral pH conditions

Both ToF-SIMS and APT data show that a small amount of boron remains – 5-20% of the glass concentration – in the alteration layer (Figure 2 in Hellmann et al. (2015) and Figure 2 of the present paper). This was also observed with ISG glass altered in silica saturated conditions at pH 7 (Gin et al., 2015a) and pH 9 (Gin et al., 2015b). As B is known to be highly soluble in these conditions, its reprecipitation is unlikely. The presence of B in the alteration layer is more likely due to small undissolved clusters. Moreover in the case of a thin interfacial film of water, APT profiles of O should dramatically change at the glass/alteration layer interface. The slight increase of O concentrations are an effect of normalization. Lastly, the presence of a thin interfacial film of water would allow the alteration layer to separate easily from the pristine glass. The mechanical tests performed by Rébiscoul showed that when the glass forms a dense alteration layer, it is not possible to separate the alteration layer from the pristine glass (Rébiscoul, 2004), which is in agreement with the fact that the silicate network does not dissolve in silica saturated solution (Gin et al., 2015a).

4.3 Importance of experimental conditions

Thirty years of research on nuclear glass alteration have shown that glass dissolution kinetics are very sensitive to temperature and chemical conditions (pH, solution composition, flow rate) as well as geometric considerations [*S*/*V*, sample preparation (grinding, polishing, cleaning), homogeneity of the solution]. If one wants to focus on chemical gradients resulting from inter-diffusion, it is required to investigate various configurations and focus on suitable designs allowing to draw unambiguous conclusion. Recently we showed that simple inter-diffusion models were not able to fit chemical gradients within hydrated glasses even in a quite simple case where pH was fixed at 7 and no secondary crystalline phase were formed (Gin et al., 2015a). This means that a better understanding on how water diffuses and reacts within nanoporous layers is necessary. Another study showed that raising the pH to 9 did not change the mechanisms but the rate of inter-diffusion was much lower (Gin et al., 2015b). However when raising the pH to 11.5, it was impossible to see evidence of inter-diffusion. In this case, like in conditions studied by Geisler et al. (2010) (pH 0, 150°C) dissolution of the glass appeared to be congruent and alteration products replacing the parent glass are formed by precipitation. These examples are taken to remind that there is no simple universal model able to account for all the cases and that the combination of all the fundamental processes involved during alteration, including inter-diffusion, have to be taken into account in predictive rate laws.

5. Conclusions

Recently, the idea of the mechanism of interfacial dissolution/precipitation has been proposed for glasses. This interpretation is based on a sharp interface observed at the pristine glass/altered interface. We have reproduced one of the key experiments used to support the interfacial dissolution/precipitation theory and have revisited the results and propose that the appearance of the interfacial dissolution/precipitation zone is strongly dependent on experimental conditions.

We end up with the following conclusions:

1) We found in the literature evidences in favor of inter-diffusion under the conditions explored by Hellmann et al., 2015. Inter-diffusion is highly favored under low temperature an acidic conditions and leads to a preferential release of alkali and boron compared to silicon.
2) We highlight the importance of experimental conditions on the glass alteration behavior. Indeed, when a low-temperature experiment is not stirred, a much smaller degree of alteration is observed compared to that expected in these highly diluted solutions. This

causes uncertainties in the local conditions near the glass surface and this is not favorable for solid characterizations.

3) For SON68 glass, inter-diffusion coefficients are of the order of 10^{-19}-10^{-21} $m^2.s^{-1}$, which correspond to solid-state diffusion. The resulting chemical gradients formed in near-neutral pH conditions (2 to 20 nm depending on the analytical technique) are small and thus difficult to characterize.
4) It is thought that when the gel is formed, inter-diffusion is limited by water accessibility to the pristine glass. The gradient area can be seen as a reactive interphase in which ion-exchange, dissolution of B-O bonds and in situ condensation reactions are taking place. By studying this zone with APT, a technique probing a 20 nm lateral area with a subnanometer depth resolution, the broader interphase described by ToF-SIMS turns into a sharper interface. This observation is consistent with inter-diffusion if one considers that the corresponding reactions create a rough interface.

References

Aagaard, P., Helgeson, H.C., 1982. Thermodynamic and kinetic constraints on reaction rates among minerals and aqueous solutions. I. Theoretical considerations. American Journal of Science, 282: 237-285.

Advocat, T., Chouchan, J.L., Ghaleb, D., Vernaz, E., 1993. Mécanismes et vitesses de dissolution initiales du verre de référence R7T7 inactif dans l'eau à 50°C, CEA Internal Report, NT/SCD/93-24.

Advocat, T., Crovisier, J.L., Vernaz, E., 1991. Aqueous corrosion of French R7T7 nuclear waste glass: selective then congruent dissolution by pH increase. Comptes Rendus de l'Académie des Sciences - Series II, 313: 407-412.

Advocat, T., Crovisier, J.L., Vernaz, E., Ehret, G., Charpentier, H., 1990. Hydrolysis of R7T7 Nuclear Waste Glass in Dilute Media: Mechanisms and Rate as a function of pH. Materials Research Society Symposium Proceedings, 212: 57-64.

Angeli, F. et al., 2001. Influence of calcium on sodium aluminosilicate glass leaching behaviour. Physics and Chemistry of Glasses, 42(4-5): 279-286.

ASTM International, 2008. Standard Test Method for Setermining Chemical Durability of Nuclear, Hazardeous, and Mixed Waste Glasses and Multiphase Glass Ceramics: The Product Consistency Test (PCT). ASTM Standard C1282-02, West Conshohocken, PA, United States.

Boksay, Z., Bouquet, G., Dobos, S., 1967. Diffusion processes in surface layers of glass. Physics and Chemistry of Glasses, 8(4): 140-144.

Bourcier, W.L., Peiffer, D.W., Knauss, K.G., McKeegan, K.D., Smith, D.K., 1989. A kinetic model for borosilicate glass dissolution affinity of a surface alteration layer. Materials Research Society Symposium Proceedings, 176: 209-216.

Bunker, B.C., 1994. Molecular mechanisms for corrosion of silica and silicate glasses. Journal of Non-Crystalline Solids, 179: 300-308.

Cailleteau, C. et al., 2008. Insight into silicate-glass corrosion mechanisms. Nature Materials, 7(12): 978-983.

Cailleteau, C., Devreux, F., Spalla, O., Angeli, F., Gin, S., 2011. Why do certain glasses with a high dissolution rate undergo a low degree of corrosion? Journal of Physical Chemistry C, 115(13): 5846-5855.

Calas, G., Brown, G., Jr., Waychunas, G., Petiau, J., 1987. X-ray absorption spectroscopic studies of silicate glasses and minerals. Physics and Chemistry of Minerals, 15(1): 19-29.

Calligan, L.J., Pierce, E.M., 2007. Experimental study of the dissolution rates of a simulated borosilicate waste glass as a function of pH and temperature. Abstracts of Papers of the American Chemical Society, 234.

Campbell, J.E., Cranwell, R.M., 1988. Performance assessment of radioactive-waste repositories. Science, 239(4846): 1389-1392.

Chamssedine, F., Sauvage, T., Peuget, S., Fares, T., Martin, G., 2010. Helium diffusion coefficient measurements in R7T7 nuclear glass by $^{3}He(d,\alpha)^{1}H$ nuclear reaction analysis. Journal of Nuclear Materials, 400(2): 175-181.

Chaou, A.A. et al., 2015. Vapor hydration of a simulated borosilicate nuclear waste glass in unsaturated conditions at 50 °C and 90 °C. RSC Advances, 5(79): 64538-64549.

Chave, T., Frugier, P., Ayral, A., Gin, S., 2007. Solid state diffusion during nuclear glass residual alteration in solution. Journal of Nuclear Materials, 362: 466-473.

Chave, T., Frugier, P., Gin, S., Ayral, A., 2011. Glass-water interphase reactivity with calcium rich solutions. Geochimica et Cosmochimica Acta, 75(15): 4125-4139.

Christie, J.K., Ainsworth, R.I., de Leeuw, N.H., 2016. Investigating structural features which control the dissolution of bioactive phosphate glasses: Beyond the network connectivity. Journal of Non-Crystalline Solids, 432: 31-34.
Conradt, R., 2008. Chemical durability of oxide glasses in aqueous solutions: A review. Journal of the American Ceramic Society, 91(3): 728-735.
Crovisier, J.L., Advocat, T., Dussossoy, J.L., 2003. Nature and role of natural alteration gels formed on the surface of ancient volcanic glasses (Natural analogs of waste containment glasses). Journal of Nuclear Materials, 321(1): 91-109.
Crovisier, J.L., Honnorez, J., Eberhart, J.P., 1987. Dissolution of basaltic glass in seawater: Mechanism and rate. Geochimica et Cosmochimica Acta, 51(11): 2977-2990.
Curti, E., Crovisier, J.L., Morvan, G., Karpoff, A.M., 2006. Long-term corrosion of two nuclear waste reference glasses (MW and SON68): A kinetic and mineral alteration study. Applied Geochemistry, 21(7): 1152-1168.
Daux, V., Guy, C., Advocat, T., Crovisier, J.-L., Stille, P., 1997. Kinetic aspects of basaltic glass dissolution at 90°C: role of aqueous silicon and aluminium. Chemical Geology, 142(1-2): 109-126.
Davis, K.M., Tomozawa, M., 1995. Water diffusion into silica glass: Structural changes in silica glass and their effect on water solubility and diffusivity. Journal of Non-Crystalline Solids, 185(3): 203-220.
Devreux, F., Ledieu, A., Barboux, P., Minet, Y., 2004. Leaching of borosilicate glasses. II. Model and Monte Carlo simulations. Journal of Non-Crystalline Solids, 343: 13-25.
Doremus, R.H., 1975. Interdiffusion of hydrogen and alkali ions in a glass surface. Journal of Non-Crystalline Solids, 19(0): 137-144.
Doremus, R.H., 1983. Diffusion-controlled reaction of water with glass. Journal of Non-Crystalline Solids, 55(1): 143-147.
Ebert, W.L., Bates, J.K., 1993. A comparison of glass reaction at high and low glass surface/solution volume. Nuclear Technology, 104(3): 372-384.
Elliott, S.R., 1991. Medium-range structural order in covalent amorphous solids. Nature, 354(6353): 445-452.
Ferrand, K., Abdelouas, A., Grambow, B., 2006. Water diffusion in the simulated French nuclear waste SON 68 contacting silica rich solutions: Experimental and modeling. Journal of Nuclear Materials, 355: 54-67.
Filgueras, M.R., Latorre, G., Hench, L.L., 1993. Solution effects on the surface reaction of bioactive glasses. Journal of Biomedical Materials Research, 27: 445-453.
Fournier, M., Frugier, P., Gin, S., 2014a. Resumption of alteration at high temperature and pH: Rates measurements and comparison with initial rates. Procedia Materials Science, 7: 202-208.
Fournier, M., Gin, S., Frugier, P., 2014b. Resumption of nuclear glass alteration: State of the art. Journal of Nuclear Materials, 448(1-3): 348-363.
Frugier, P., Chave, T., Gin, S., Lartigue, J.E., 2009. Application of the GRAAL model to leaching experiments with SON68 nuclear glass in initially pure water. Journal of Nuclear Materials, 392(3): 552-567.
Frugier, P. et al., 2008. SON68 nuclear glass dissolution kinetics: Current state of knowledge and basis of the new GRAAL model. Journal of Nuclear Materials, 380(1-3): 8-21.
Frugier, P., Martin, C., Ribet, I., Advocat, T., Gin, S., 2005. The effect of composition on the leaching of three nuclear waste glasses: R7T7, AVM and VRZ. Journal of Nuclear Materials, 346(2-3): 194-207.

Galeczka, I., Wolff-Boenisch, D., Oelkers, E.H., Gislason, S.R., 2014. An experimental study of basaltic glass–H_2O–CO_2 interaction at 22 and 50 °C: Implications for subsurface storage of CO_2. Geochimica et Cosmochimica Acta, 126: 123-145.
Geisler, T. et al., 2010. Aqueous corrosion of borosilicate glass under acidic conditions: A new corrosion mechanism. Journal of Non-Crystalline Solids, 356(28-30): 1458-1465.
Geisler, T. et al., 2015. The mechanism of borosilicate glass corrosion revisited. Geochimica et Cosmochimica Acta, 158: 112-129.
Gin, S. et al., 2013a. An international initiative on long-term behavior of high-level nuclear waste glass. Materials Today, 16(6): 243-248.
Gin, S., Beaudoux, X., Angéli, F., Jégou, C., Godon, N., 2012. Effect of composition on the short-term and long-term dissolution rates of ten borosilicate glasses of increasing complexity from 3 to 30 oxides. Journal of Non-Crystalline Solids, 358(18-19): 2559-2570.
Gin, S., Frugier, P., Jollivet, P., Bruguier, F., Curti, E., 2013b. New Insight into the Residual Rate of Borosilicate Glasses: Effect of S/V and Glass Composition. International Journal of Applied Glass Science, 4(4): 371-382.
Gin, S. et al., 2011. Nuclear Glass Durability: New Insight into Alteration Layer Properties. Journal of Physical Chemistry C, 115(38): 18696-18706.
Gin, S. et al., 2015a. Origin and consequences of silicate glass passivation by surface layers. Nature Communications, 6.
Gin, S. et al., 2015b. The fate of silicon during glass corrosion under alkaline conditions: A mechanistic and kinetic study with the International Simple Glass. Geochimica et Cosmochimica Acta, 151: 68-85.
Gin, S., Mestre, J.P., 2001. SON 68 nuclear glass alteration kinetics between pH 7 and pH 11.5. Journal of Nuclear Materials, 295(1): 83-96.
Gin, S., Ribet, I., Couillard, M., 2001. Role and properties of the gel formed during nuclear glass alteration: Importance of gel formation conditions. J. Nucl. Mater., 298: 1-10.
Gin, S., Ryan, J.V., Schreiber, D.K., Neeway, J., Cabié, M., 2013c. Contribution of atom-probe tomography to a better understanding of glass alteration mechanisms: Application to a nuclear glass specimen altered 25 years in a granitic environment. Chemical Geology, 349-350: 99-109.
Grambow, B., 1985. A general rate equation for nuclear waste glass corrosion. Materials Research Society Symposium Proceedings, 44: 15-27.
Grambow, B., 2006. Nuclear waste glasses; how durable? Elements, 2(6): 357-364.
Grambow, B., Müller, R., 2001. First-order dissolution rate law and the role of surface layers in glass performance assessment. Journal of Nuclear Materials, 298(1-2): 112-124.
Hellmann, R. et al., 2015. Nanometre-scale evidence for interfacial dissolution–reprecipitation control of silicate glass corrosion. Nature Materials, 14(3): 307-311.
Hellmann, R. et al., 2012. Unifying natural and laboratory chemical weathering with interfacial dissolution–reprecipitation: A study based on the nanometer-scale chemistry of fluid–silicate interfaces. Chemical Geology, 294-295: 203-216.
Hench, L.L., 2006. The story of Bioglass (R). Journal of Materials Science-Materials in Medicine, 17(11): 967-978.
Hench, L.L., Clark, D.E., 1978. Physical chemistry of glass surface. J. Non-Cryst. Solids, 28: 83-105.

Icenhower, J.P., Steefel, C.I., 2013. Experimentally determined dissolution kinetics of SON68 glass at 90°C over a silica saturation interval: Evidence against a linear rate law. Journal of Nuclear Materials, 439(1-3): 137-147.
Iler, R.K., 1979. The Chemistry of Silica: Solubility, Polymerization, Colloid and Surface Properties, and Biochemistry of Silica. John Wiley & Sons Inc.
Inagaki, Y., Kikunaga, T., Idemitsu, K., Arima, T., 2013. Initial dissolution rate of the International Simple Glass as a function of pH and temperature measured using microchannel flow-through test method. International Journal of Applied Glass Science, 4(4): 317-327.
Jégou, C., Gin, S., Larché, F., 2000. Alteration kinetics of a simplified nuclear glass in an aqueous medium: effects of solution chemistry and of protective gel properties on diminishing the alteration rate. Journal of Nuclear Materials, 280(2): 216-229.
Jollivet, P. et al., 2008. Investigation of gel porosity clogging during glass leaching. Journal of Non-Crystalline Solids, 354(45-46): 4952-4958.
Jollivet, P., Gin, S., Schumacher, S., 2012. Forward dissolution rate of silicate glasses of nuclear interest in clay-equilibrated groundwater. Chemical Geology, 330-331: 207-217.
Kerisit, S., Pierce, E.M., Ryan, J.V., 2015. Monte Carlo simulations of coupled diffusion and surface reactions during the aqueous corrosion of borosilicate glasses. Journal of Non-Crystalline Solids, 408: 142-149.
Knauss, K.G. et al., 1989. Dissolution Kinetics of a Simple Analogue Nuclear Waste Glass as a Function of pH, Time and Temperature. Materials Research Society Symposium Proceedings, 176: 371-381.
Knowles, E., Wirth, R., Templeton, A., 2012. A comparative analysis of potential biosignatures in basalt glass by FIB-TEM. Chemical Geology, 330–331: 165-175.
Kokubo, T., 1991. Bioactive glass-ceramics - Properties and applications. Biomaterials, 12(2): 155-163.
Ledieu, A., Devreux, F., Barboux, P., Sicard, L., Spalla, O., 2004. Leaching of borosilicate glasses. I. Experiments. Journal of Non-Crystalline Solids, 343: 3-12.
Leturcq, G., Berger, G., Advocat, T., Vernaz, E., 1999. Initial and long-term dissolution rates of aluminosilicate glasses enriched with Ti, Zr and Nd. Chemical Geology, 160(1-2): 39-62.
Libourel, G. et al., 2011. The use of natural and archeological analogues for understanding the long-term behavior of nuclear glasses. Comptes Rendus Geoscience, 343(2-3): 237-245.
Maeda, T., Hotta, K., Usui, H., Banda, T., 2012. Characteristics of Alteration Layers Formed on Simulated HLW Glass under Silica-saturated Solutions. Journal of the Australian Ceramics Society 48: 90-95.
McGrail, B.P. et al., 2001. The structure of Na_2O–Al_2O_3–SiO_2 glass: impact on sodium ion exchange in H_2O and D_2O. Journal of Non-Crystalline Solids, 296(1-2): 10-26.
Minitti, M.E., Weitz, C.M., Lane, M.D., Bishop, J.L., 2007. Morphology, chemistry, and spectral properties of Hawaiian rock coatings and implications for Mars. Journal of Geophysical Research-Planets, 112(E5).
Morin, G.P., Vigier, N., Verney-Carron, A., 2015. Enhanced dissolution of basaltic glass in brackish waters: Impact on biogeochemical cycles. Earth and Planetary Science Letters, 417: 1-8.
Munier, I., Crovisier, J.L., 2003. Alteration of Si-B-Na-Al model glass in water at 90 °C: experiments and thermodynamic modelling. Materials Research Society Symposium Proceedings, 757: 153-158.

Ojovan, M., Lee, W., 2011. Glassy Wasteforms for Nuclear Waste Immobilization. Metallurgical and Materials Transactions A: Physical Metallurgy and Materials Science, 42(4): 837-851.
Ojovan, M.I., Pankov, A., Lee, W.E., 2006. The ion exchange phase in corrosion of nuclear waste glasses. Journal of Nuclear Materials, 358(1): 57-68.
Ostwald, W., 1897. Studien über die Bildung und Umwandlung fester Körper. Zeitschrift für Physikalische Chemie, 22: 289-330.
Parruzot, B., Jollivet, P., Rébiscoul, D., Gin, S., 2015. Long-term alteration of basaltic glass: Mechanisms and rates. Geochimica et Cosmochimica Acta, 154: 28-48.
Petit, J.C., Magonthier, M.C., Dran, J.C., Mea, G.D., 1990a. Long-term dissolution rate of nuclear glasses in confined environments: does a residual chemical affinity exist? Journal of Materials Science, 25(7): 3048-3052.
Petit, J.C. et al., 1990b. Hydrated-layer formation during dissolution of complex silicate glasses and minerals. Geochimica et Cosmochimica Acta, 54(7): 1941-1955.
Pierce, E.M., Bacon, D.H., 2011. Combined experimental and computational approach to predict the glass-water reaction. Nuclear Technology, 176(1): 22-39.
Pierce, E.M., Rodriguez, E.A., Calligan, L.J., Shaw, W.J., McGrail, B.P., 2008. An experimental study of the dissolution rates of simulated aluminoborosilicate waste glasses as a function of pH and temperature under dilute conditions. Applied Geochemistry, 23(9): 2559-2573.
Poinssot, C., Gin, S., 2012. Long-term Behavior Science: The cornerstone approach for reliably assessing the long-term performance of nuclear waste. Journal of Nuclear Materials, 420(1-3): 182-192.
Rajmohan, N., Frugier, P., Gin, S., 2010. Composition effects on synthetic glass alteration mechanisms: Part 1. Experiments. Chemical Geology, 279(3-4): 106-119.
Rébiscoul, D., 2004. Etude de la pérennité des gels d'altération des verres nucléaires, PhD thesis, Montpellier 2 University, France.
Rébiscoul, D., Bruguier, F., Magnin, V., Gin, S., 2012. Impact of soda-lime borosilicate glass composition on water penetration and water structure at the first time of alteration. Journal of Non-Crystalline Solids, 358(22): 2951-2960.
Rébiscoul, D., Frugier, P., Gin, S., Ayral, A., 2005. Protective properties and dissolution ability of the gel formed during nuclear glass alteration. Journal of Nuclear Materials, 342(1-3): 26-34.
Rébiscoul, D. et al., 2007. Water penetration mechanisms in nuclear glasses by X-ray and neutron reflectometry. Journal of Non-Crystalline Solids, 353(22-23): 2221-2230.
Rebiscoul, D., van der Lee, A., Frugier, P., Ayral, A., Gin, S., 2003. X-ray reflectometry characterization of SON 68 glass alteration films. Journal of Non-Crystalline Solids, 325(1-3): 113-123.
Rébiscoul, D. et al., 2004. Morphological evolution of alteration layers formed during nuclear glass alteration: new evidence of a gel as a diffusive barrier. Journal of Nuclear Materials, 326(1): 9-18.
Ribet, S., Gin, S., 2004. Role of neoformed phases on the mechanisms controlling the resumption of SON68 glass alteration in alkaline media. Journal of Nuclear Materials, 324(2-3): 152-164.
Santra, S.B., Sapoval, B., Barboux, P., Devreux, F., 1998. Pseudo-equilibrium between a random system and a solution: a Monte-Carlo study of glass dissolution in water. Comptes Rendus de l'Académie des Sciences - Series IIB: Mechanics, Physics, Chemistry, Astronomy, 326(2): 129-134.

Seyfried Jr, W.E., Janecky, D.R., Mottl, M.J., 1984. Alteration of the oceanic crust: Implications for geochemical cycles of lithium and boron. Geochimica et Cosmochimica Acta, 48(3): 557-569.
Smets, B.M.J., Lommen, T.P.A., 1983. The role of molecular water in the leaching of glass. Physics and Chemistry of Glasses, 24(1): 35-36.
Stebbins, J.F., Xu, Z., 1997. NMR evidence for excess non-bridging oxygen in an aluminosilicate glass. Nature, 390(6655): 60-62.
Strachan, D.M., Neeway, J.J., 2014. Effects of alteration product precipitation on glass dissolution. Applied Geochemistry, 45: 144-157.
Techer, I., Advocat, T., Lancelot, J., Liotard, J.-M., 2000. Basaltic glass: alteration mechanisms and analogy with nuclear waste glasses. Journal of Nuclear Materials, 282(1): 40-46.
Techer, I., Advocat, T., Lancelot, J., Liotard, J.-M., 2001. Dissolution kinetics of basaltic glasses: control by solution chemistry and protective effect of the alteration film. Chemical Geology, 176(1-4): 235-263.
Threlfall, T., 2003. Structural and thermodynamic explanations of Ostwald's rule. Organic Process Research & Development, 7(6): 1017-1027.
Valle, N. et al., 2010. Elemental and isotopic (^{29}Si and ^{18}O) tracing of glass alteration mechanisms. Geochimica et Cosmochimica Acta, 74(12): 3412-3431.
Van Iseghem, P. et al., 2009. GLAMOR - Or how we achieved a common understanding on the decrease of glass dissolution kinetics. Ceramic Transactions, 207(s): 115-126.
Vernaz, E.Y., Dussossoy, J.L., 1992. Current state of knowledge of nuclear waste glass corrosion mechanisms: the case of R7T7 glass. Applied Geochemistry, 7, Supplement 1: 13-22.
Verney-Carron, A., Gin, S., Libourel, G., 2008. A fractured roman glass block altered for 1800 years in seawater: Analogy with nuclear waste glass in a deep geological repository. Geochimica et Cosmochimica Acta, 72(22): 5372-5385.
Vienna, J.D., Ryan, J.V., Gin, S., Inagaki, Y., 2013. Current understanding and remaining challenges in modeling long-term degradation of borosilicate nuclear waste glasses. International Journal of Applied Glass Science, 4(4): 283-294.
Werme, L.O., Hench, L.L., Nogues, J.L., Odelius, H., Lodding, A., 1983. On the pH dependence of leaching of nuclear waste glasses. Journal of Nuclear Materials, 116(1): 69-77.
Zachariasen, W.H., 1932. The atomic arrangement in glass. Journal of the American Chemical Society, 54: 3841-3851.
Zapol, P., He, H., Kwon, K.D., Criscenti, L.J., 2013. First-Principles Study of Hydrolysis Reaction Barriers in a Sodium Borosilicate Glass. International Journal of Applied Glass Science, 4(4): 395-407.

Acknowledgements

This work was initiated during the visit of Lindsey Neill, PhD student at Washington State University and recipient of the 2014 Chateaubriand Fellowship, at CEA Marcoule from September 2014 to June 2015. Authors are grateful to CEA, Areva, and the Embassy of France in the U.S. for the financial support.

Figures

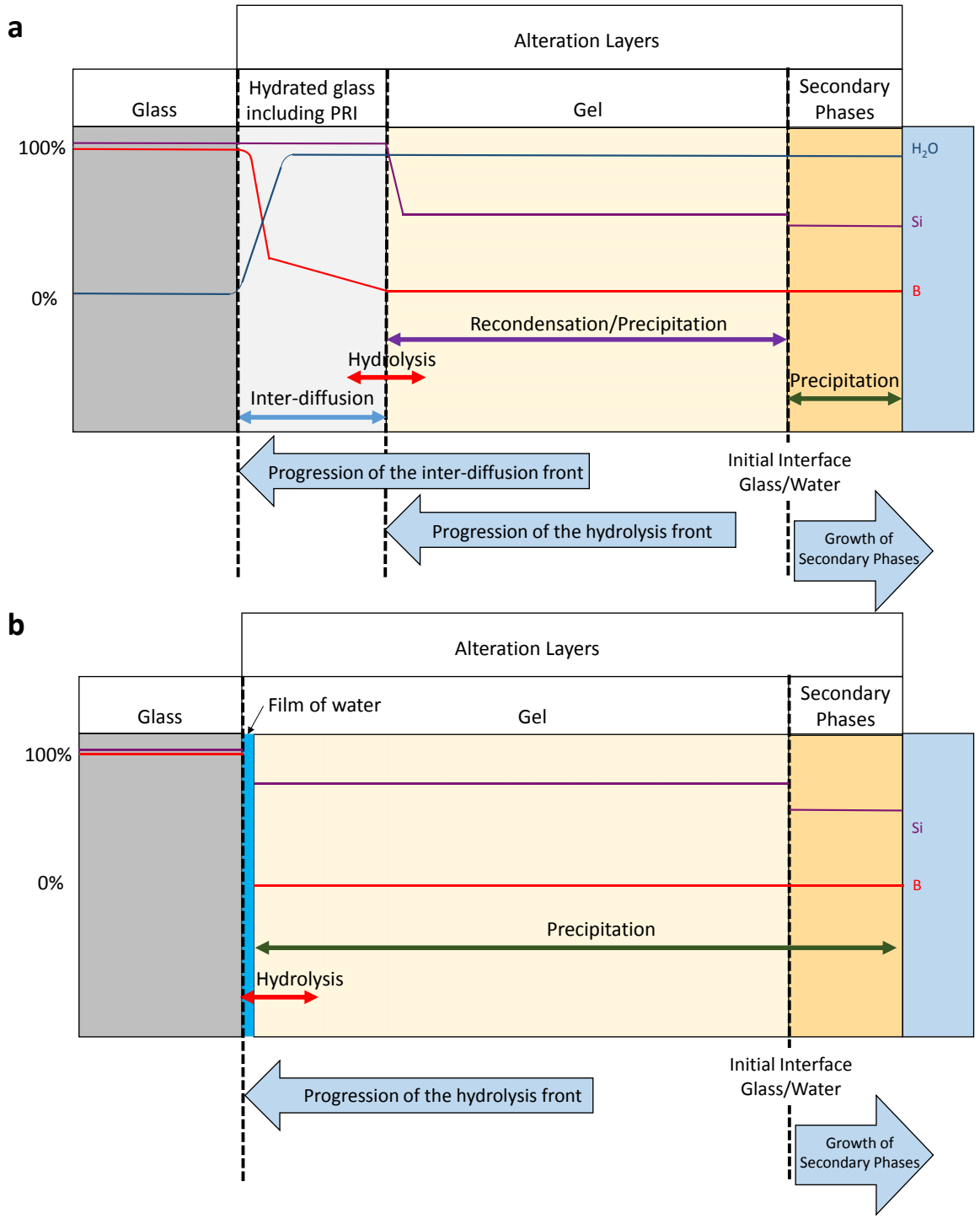

Figure 1: Sketch showing the layers formed during SON68 glass alteration: a) according to the classical theory including inter-diffusion and b) according the interfacial dissolution-precipitation model. The thickness of each layer is indicative. It depends on the experimental conditions (temperature, pH, solution composition, flow rate).

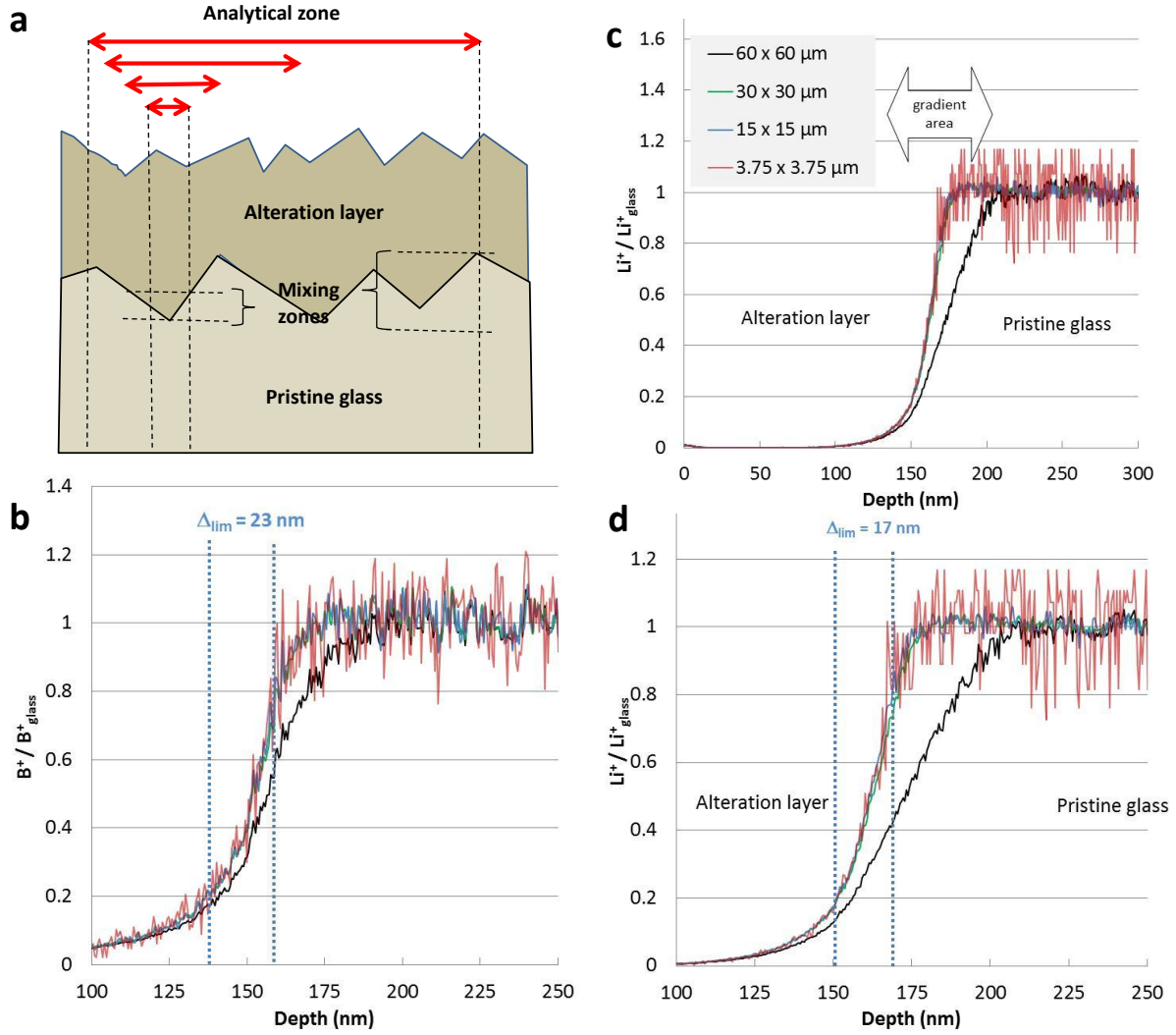

Figure 2: TOF-SIMS analysis of 180 day monolith. Chemical profiles are calculated in areas of 30 x 30 µm, 15 x 15 µm, 7.5 x 7.5 µm and 3.75 x 3.75 µm within the 60 x 60 µm area for boron (b) and lithium (c, d). This helps identify the existence of a mixing zone due to a rough interface or an uneven alteration layer (a).

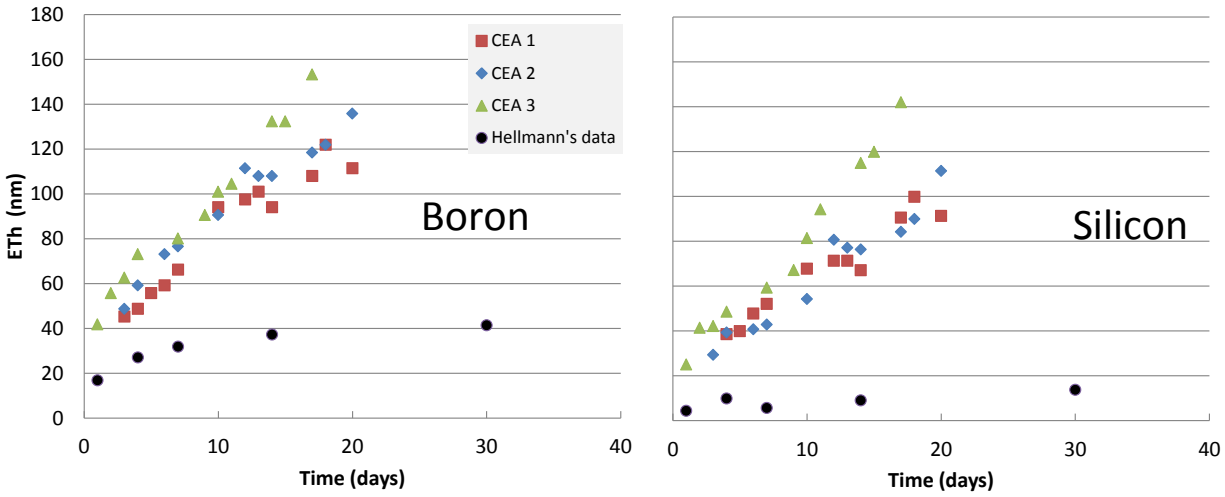

Figure 3: Equivalent thickness *ETh* of altered glass calculated from B (left) and Si (right). Here we compare results from a series of 3 experiments conducted at CEA in the 1990s with that obtained in Hellmann et al. (Hellmann et al., 2015). Both type of experiments were performed at 50°C, low *S/V* (0.24 cm^{-1} for CEA's experiments and 0.1 cm^{-1} for Hellmann's experiment). Solution was stirred in CEA experiments and not for the Hellmann's experiment.

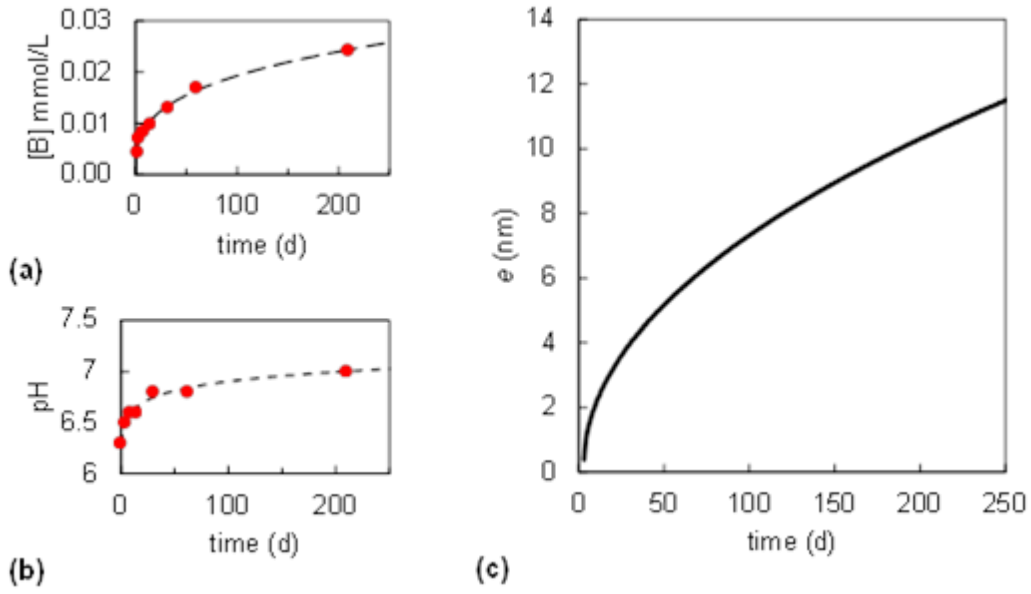

Figure 4: Evolutions of boron concentration (a) and pH (b) are derived from Hellmann *et al*., 2015 data. Experimental data are fitted with power laws in order to calculate a continuous evolution of the thickness *e* of the diffusion zone versus time according to equation 9.

Tables

Table 1: Composition of SON68 glass

Oxide	mol%	Oxide	mol%	Oxide	mol%
SiO_2	52.72	MoO_3	0.85	CdO	0.02
Al_2O_3	3.39	Cs_2O	0.28	SnO_2	0.01
B_2O_3	14.03	NiO	0.4	TeO_2	0.1
Na_2O	11.39	P_2O_5	0.14	BaO	0.28
CaO	5.02	SrO	0.23	La_2O_3	0.2
Li_2O	4.6	Cr_2O_3	0.24	Ce_2O_3	0.2
ZnO	2.15	Y_2O_3	0.06	Pr_2O_3	0.1
ZrO_2	1.54	MnO_3	0.31	La_2O_3	0.42
Fe_2O_3	1.31	Ag_2O	0.01		

Table 2: Diffusion coefficients measured for SON68 or similar glasses at low and high reaction progress.

Element	Glass Type	Method	*D* $m^2.s^{-1}$	Remarks	Source
Low Reaction Progress: Far from Saturated Conditions					
Water	simple borosilicate	XRR	10^{-19} - 10^{-21}	12 °C - 60 °C	Rebiscoul et al., 2012
Water	SON68	XRR	6.5×10^{-21}	50 °C pH 5.7	Rebiscoul et al., 2007
Li^+	SON68	TOF-SIMS	$2.0 - 4.0 \times 10^{-21}$	90°C Non aqueous medium	Neeway et al., 2014
Na^+	SON68	TOF-SIMS	$1.0 - 2.0 \times 10^{-20}$	90°C Non aqueous medium	Neeway et al., 201
High Reaction Progress: Near Saturated Conditions					
Water	SON68	APT	6.8×10^{-23}	25 year alterated glass at 90 °C	Gin et al., 2013b
Water	SON68	Solution Analysis	10^{-22} - 10^{-24}	50 °C pH 5 - 10	Ferrand et al., 2006
Water	SON68	Solution Analysis	10^{-21} - 10^{-23}	90 °C pH 5 - 10	Ferrand et al., 2006
Li^+	SON68	APT	1.5×10^{-22}	25 year alterated glass at 90 °C	Gin et al., 2013b
Na^+	P0798	Solution Analysis	4.1×10^{-23}	60 °C	Maeda et al., 2012

Table 3: Solution data (pH and ICP-OES analysis) for our test and for the test reported in Hellmann et al., 2015.

Days	pH - This study	pH - Hellmann	[Si] ppm This Study	[Si] ppm Hellmann	[B] ppm This Study	[B] ppm Hellmann
1	7.1 ± 0.5	6.3	0.43 ± 0.40	0.06	0.02 ± 0.01	0.05
4	6.8 ± 1.0	6.5	0.85 ± 0.93	0.14	0.05 ± 0.03	0.08
7	6.7 ± 0.4	6.6	0.61 ± 1.07	0.08	0.06 ± 0.00	0.09
14	6.9 ± 0.4	6.6	0.89 ± 1.31	0.13	0.09 ± 0.01	0.11
30	6.8 ± 0.3	6.8	1.34 ± 1.01	0.19	0.14 ± 0.03	0.14